www.ptcer.pl/mccm

MATERIAŁY CERAMICZNE /CERAMIC MATERIALS/, 69, 3, (2017), 279-285

Mechanical properties and low temperature degradation resistance of alumina-doped 3Y-TZP fabricated from stabilizer coated powders

Frank Kern[1]*, Ahsanul Kabir[1,2], Rainer Gadow[1]

[1]Universität Stuttgart, IFKB, Allmandring 7B, D-70569 Stuttgart, Germany
[2]Department of Energy Conversation and Storage, Technical University of Denmark (DTU), DK-4000 Roskilde, Denmark
*e-mail: frank.kern@ifkb.uni-stuttgart.de

Abstract

In this study nanoscale monoclinic zirconia was coated with 3 mol % yttria via the nitrate route. Up to 2 vol.% of alumina were added by either coating or mixing and milling. The mechanical properties of the materials, microstructure and phase composition were studied. Low temperature degradation resistance was determined by an accelerated autoclave test. The TZP materials showed a high toughness of > 10 MPa√m combined with a strength of ~ 740-1000 MPa. Low temperature degradation resistance improved with alumina addition, here the introduction of alumina by mixing and milling was more efficient than by powder coating; the maximum monoclinic fraction in the mixed composite was only 6 vol.% after 100 h of autoclave ageing at 134 °C and the monoclinic phase did not form a fully connected layer.

Keywords: 3Y-TZP, Law temperature degradation, Coating, Microstructure final, Mechanical properties

WŁAŚCIWOŚCI MECHANICZNE I ODPORNOŚĆ NA NISKOTEMPERATUROWĄ DEGRADACJĘ DOMIESZKOWANEGO TLENKIEM GLINU 3Y-TZP, WYTWORZONEGO Z PROSZKÓW POKRYWANYCH STABILIZATOREM

W niniejszym badaniu jednoskośny nanometryczny dwutlenek cyrkonu pokrywano tlenkiem itru w ilości 3% mol., wykorzystując ścieżkę azotanową. Poprzez pokrywanie lub mieszanie i mielenie dodano aż do 2% obj. tlenku glinu. Zbadano właściwości mechaniczne, mikrostrukturę i skład fazowy materiałów. Za pomocą przyśpieszonego testu autoklawowego określono niskotemperaturową degradację. Materiały TZP pokazały wysoką odporność na pękanie przekraczającą 10 MPa√m w połączeniu z wytrzymałością wynoszącą ~740-1000 MPa. Odporność na niskotemperaturową degradację została poprawiona dodatkiem tlenku glinu, gdzie wprowadzenie tlenku glinu drogą mieszania i mielenia było bardziej efektywne niż przez pokrywanie proszku; maksymalna frakcja jednoskośnia w kompozycie stanowiła jedynie 6% obj. po starzeniu w autoklawie przez 100 h w 134 °C, a faza jednoskośna nie utworzyła całkowicie spójnej warstwy.

Słowa kluczowe: 3-YTZ, degradacja niskotemperaturowa, pokrywanie, mikrostruktura finalna, właściwości mechaniczne

1. Introduction

Yttria stabilized zirconia was introduced in the late 1970s and has since then become one of the most frequently applied structural ceramics for applications at ambient temperature due to its high strength and fracture resistance [1-3]. These favorable mechanical properties are the result of the transformation toughening effect. At the tip of a proceding crack metastable tetragonal zirconia transforms to thermodynamically stable monoclinic form. This martensitic phase transformation is associated with volume expansion and shear, the resulting compressive stress on the crack stops or retards crack extension [4]. As the phase transformations are fully reversible with changes in temperature, stabilizer oxides such as magnesia or yttria are added to retain the tetragonal phase metastable after cooling to room temperature [5]. The typical Y-TZP contains 3 mol% Y_2O_3, and thus has a composition in the t+c field (a miscibility gap). Two solids are coexisting (~80% tetragonal and ~20% cubic) in thermodynamic equilibrium at sintering temperature of ~1400 °C [6]. The stabilizing effect of trivalent Y^{3+} cations is due to the introduction of oxygen vacancies to retain charge neutrality. In the tetragonal solid solution yttrium cations are in eightfold, zirconium cations in sevenfold coordination [7].

The metastability of the tetragonal phase, which is beneficial for high toughness, however, also leads the major drawback of Y-TZP, low temperature degradation (LTD). Exposed to water, hydroxide ions can enter oxygen vacancies and destabilize the tetragonal phase. Once the phase transformation has started, it proceeds into the bulk of the material as grains suffer from volume expansion and leave the grain boundaries under stress. Comprehensive studies on the LTD have been published by Chevalier and Keuper [8-11]. The tetragonal phase of typical alumina free 3Y-TZP

made from co-precipitated powder almost entirely transforms to monoclinic in 10 h in an accelerated ageing test at 130 °C (1 h in autoclave ~ 3 years in vivo). Alumina addition improves the ageing resistance of Y-TZP as alumina is incorporated into the boundaries of the Y-TZP grains [12]. Piconi and Burger found that 3Y-TZP made from stabilizer coated powder shows considerably higher ageing stability [13]. Recent results by Zhang have confirmed these findings [14]. Besides boosting the LTD resistance the coating process potentially improves the fracture resistance. Early studies by Singh and Burger [15, 16] and some own investigations [17] have led to very tough materials, the 3Y-TZPs by Zhang based on Tosoh TZ-0, however, only showed moderate toughness values slightly higher than standard material [14]. With regard to recent findings by Danilenko [18] who found very high toughness in 3Y-TZP, in which alumina was introduced by co-precipitation, it was tried to elucidate how the procedure of alumina addition affects the mechanical and ageing characteristics of 3Y-TZP. The materials development aims at obtaining strong tough and reliable Y-TZP materials operating under influence of moisture for e.g. for biomedical applications. Moreover these materials may applied as a matrix in various TZP based composite ceramics for mechanical engineering applications.

2. Experimental

The powder coating process basically followed the nitrate route developed by Yuan [19]. The starting powder for this study was an unstabilized zirconia nanopowder (S_{BET} = 15 m²/g). An appropriate amount of yttria (99.9% purity) to adjust the Y_2O_3 content in the final Y-TZP powder to 3 mol% was dissolved in boiling 5N nitric acid. The zirconia was dispersed in 2-propanol and the cooled yttrium nitrate solution was added. The first batch was plain 3Y-TZP (0Al), in the second batch 2 vol.% alumina were introduced by addition of aluminium nitrate nonahydrate (99.9% purity) to the yttrium nitrate solution (2Al-C). In the third batch the 2 vol.% alumina (S_{BET} = 8 m²/g) were added to the 3Y-TZP by mixing and milling after the powder coating process (2Al-M). The dispersions were milled overnight in a PE bottle (containing 500 g powder, 1000 g 3Y-TZP milling balls (d = 2 mm) and 1500 ml 2-Propanol). The milling balls were separated and the suspension was first dried 90 °C and pre-calcined at 350 °C for 3 h in air. Then the powder was crushed and sieved (100 µm). After final calcination at 600 °C for 3 h in air, the powders were attrition milled in 2 propanol with 2 mm Y-TZP balls for 2 h at 500 rpm. The powders were again dried at 90 °C in air and sieved (100 µm). Samples were obtained by hot pressing (FCT Anlagenbau, Germany) in boron nitride clad graphite dies (d = 45 mm) in vacuum at a temperature of 1350 °C and a dwell of 1 h at an axial pressure of 50 MPa. Four disks (height 2.5 mm) of each composition were pressed. The disks were subsequently lapped with 15 µm diamond suspension and polished with 15 µm, 6 µm and 1µm suspension to a mirror-like finish (Struers Rotopol, Denmark). Two disks of each type were cut into bending bars of 4 mm width (Struers Accutom, Denmark). Sides and edges of the bending bars were lapped and bevelled to remove machining defects.

The calcined and milled powders were studied by TEM (Zeiss Libra, Germany). The mechanical characterization of the samples included measurement of Vickers hardness HV10 (Bareiss, Germany, 5 indents each), four point bending strength (Zwick, Germany, outer/inner span 20/10 mm, crosshead speed 0,5 mm/min, 10 samples each) measurement of fracture resistance by the ISB method (same setup, crosshead speed 2.5 mm/min, 4 samples each). For the ISB test the samples were notched with a HV10 indent in the middle of the tensile side with cracks parallel and perpendicular to the sides prior to testing, the calculation of toughness was carried out according to Chantikul [20]. The resistance to subcritical crack growth/ threshold toughness was determined according to Dransmann by stable indentation crack growth in bending [21]. Based on examinations of the indentation crack geometry, a more realistic value of Ψ = 1.05 was used instead of the ideal crack geometry factor Ψ = 1.27 [21]. Density by the buoyancy method and measurement of Young's modulus (IMCE, Belgium) were carried out on entire polished disks.

The microstructure of the samples was studied by SEM (Zeiss Gemini, Germany, in lens secondary electrons), Polished surfaces were thermally etched in hydrogen (1175 °C, 5 min) to reveal the grain boundaries; fracture faces after bending test were also examined. The grain sizes were determined by the line intercept method using a minimum of 100 grains; the grain sizes were corrected by multiplying the average measured grain size by 1.57 [22].

The accelerated ageing test was carried out by exposing polished samples of ~ 10 mm × 10 mm × 2 mm to saturated water vapour in an autoclave (Roth, Germany) at 134 °C under 3 bar for 1-100 h. The aged surfaces were studied by white light interferometry (Bruker, Germany). The monoclinic phase content of polished, fractured and hydrothermally aged samples was studied by XRD (Panalytical, Japan, Bragg-Brentano setup, CuKα) by integrating the intensities of the characteristic $(\bar{1}11)_m$, $(111)_m$ and $101)_t$ peaks in the 27–32° 2Θ-range and calculating monoclinic fractions according to the calibration curve of Toraya [23]. For the determination of the relevant coefficients of the nucleation and growth kinetics of monoclinic formation and progression into the bulk a Mehl-Avrami-Johnson (MAJ) kinetics is assumed (Eq. 1) [8]:

$$V_m = 1 - e^{(-bt)^m} \quad (1)$$

The coefficients are the rate constant b and the Avrami-Exponent (nucleation factor) m, this exponential expression can be linearized by plotting $\ln(\ln(1/(1-V_m)))$ versus $\ln t$. This MAJ-plot delivers the ordinate intercept $\ln b$ and the slope m.

3. Results

3.1. Characterization of coated powders

The morphology of coated 3Y-TZP powders is shown in Fig. 1. The zirconia nanopowder has a relatively broad size distribution. Crystallite sizes range from 20-150 nm. The powder is soft agglomerated. Neither images of 0Al

nor 2Al-C powder show indications of the yttria or yttria-alumina coating.

3.2. Mechanical properties

The mechanical properties of the three TZP materials are shown in Table 1. All samples are completely dense. The values of hardness and Young's modulus are in the typical range for 3Y-TZP materials. The bending strength values of ~1000 MPa for 0Al and 2AL-M are typical values for 3Y-TZP, the low strength of the 2Al-C is however an indication of large defects. The plain 3Y-TZP (0Al) has the lowest toughness K_{IC} of 10 MPa√m, the toughness of the two alumina doped TZP materials is considerably higher and reaches a maximum value of 12 MPa√m for the 2Al-M. The residual strength of *HV*10 indented 2Al-C bars of 650-700 MPa is close to the bending strength, it may thus well be that the real toughness of 2Al-C is actually higher but cannot be determined by ISB-Test.

Compared to standard 3Y-TZP, which typically has a K_{IC} of 5-6 MPa√m, the fracture resistance of all three materials is outstanding. The threshold toughness in the range between 5.8-6.6 MPa√m is much higher than in case of coprecipitated 3Y-TZP (2.8-3 MPa√m [24]), alumina doped materials show a higher threshold toughness K_{I0}. Threshold toughness values determined here are in the range of the values observed in an earlier publication on 2.5Y-TZP-alumina composites [25].

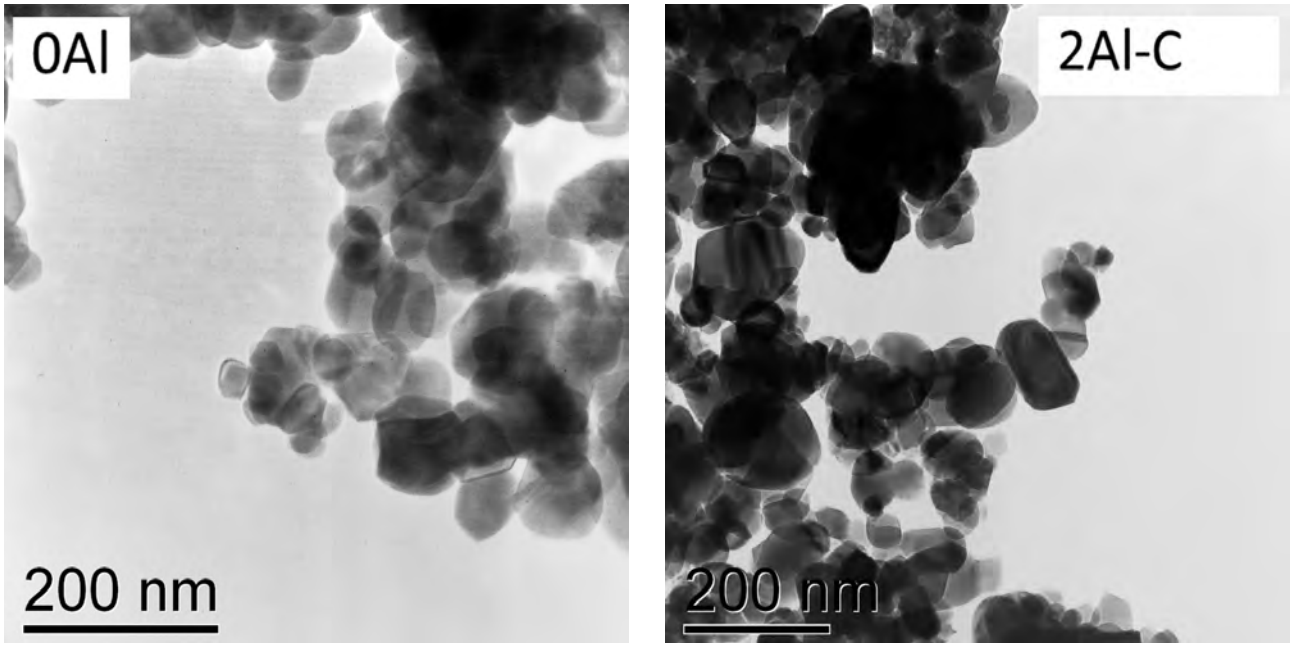

a) b)

Fig. 1. Bright field TEM images of TZP powders 0Al (a) and 2Al-C (b) after calcination and milling.

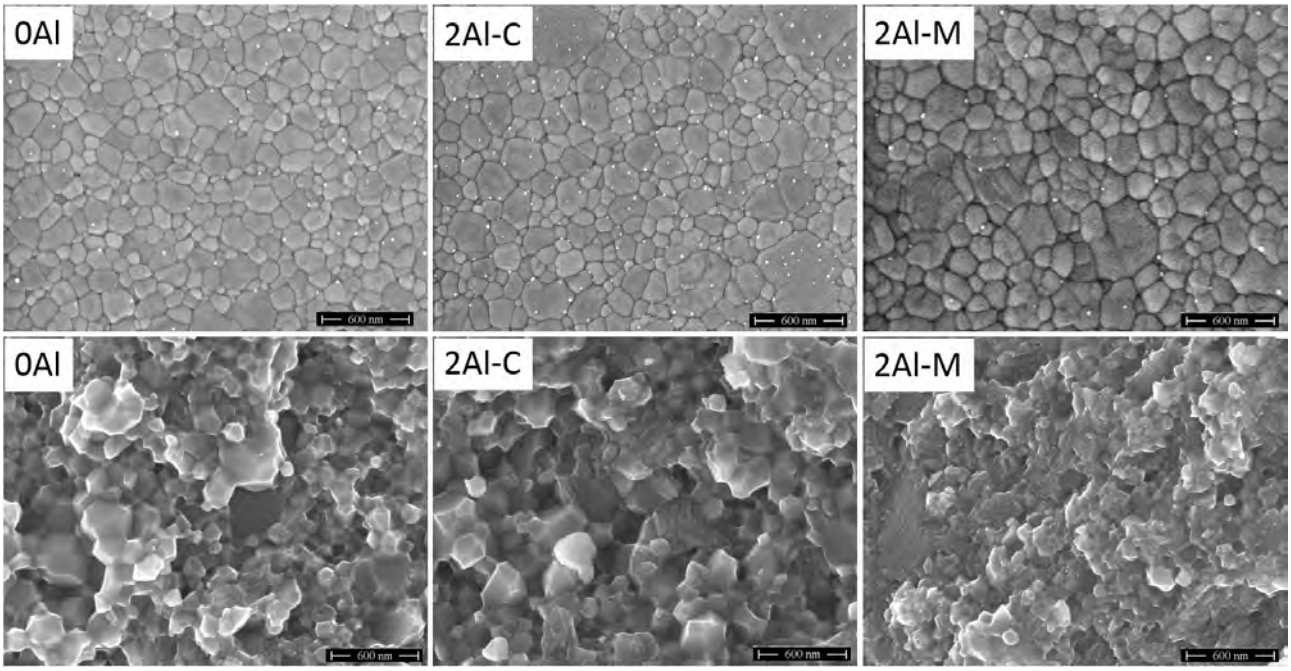

Fig. 2. SEM images of thermally etched surfaces and fracture faces.

3.3. Microstructure

Fig. 2 shows the microstructure of thermally etched materials together with the structure of fracture faces. The microstructure of all three materials is very fine grained. Average grain sizes are 180 ± 20 nm for 0Al, 210 ± 20 nm for 2Al-C and 160 nm for 2Al-M. In all three materials, there are a few larger grains of 1µm size visible which are presumably cubic.

Evidently the fracture mode changes considerably with alumina addition. In case of the alumina-free 0Al, the material shows the typical predominantly intergranular fracture behaviour of 3Y-TZP. In 2Al-C, the material with the alumina introduced by coating shows inter- and transgranular fracture in equal ratio. In 2Al-M transgranular fracture is dominant. Fig. 3 shows a detail from the fracture face of 2Al-C. It seems that in 2Al-C the alumina is not evenly distributed. Alumina seems to segregate during the powder conditioning presumably during drying or calcination. The large alumina inclusions always show transgranular conchoidal fracture. In some cases, the core of these regions contains well crystallized plate shaped precipitates of α-alumina within a poorly crystallized shell which presumably consists of transition alumina. The low calcination and heat treatment temperatures and short dwell seem to be insufficient to transform the alumina completely to α-phase. The size of these brittle alumina inclusions may be the reason for the poor strength of 2Al-C. Some cracks which may act as critical defects are visible around the alumina precipitates.

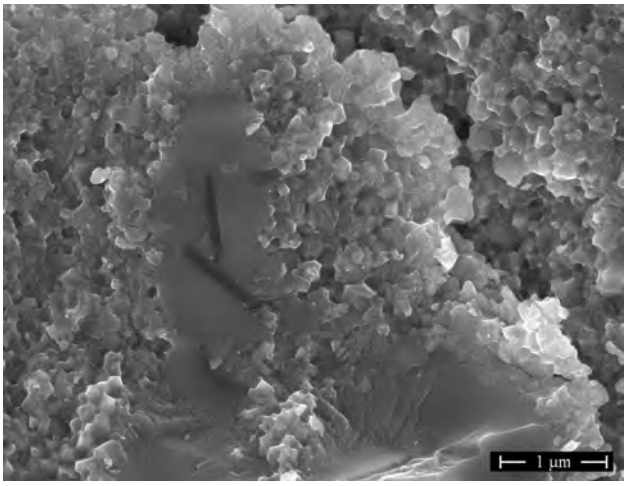

Fig. 3. 2Al-C; SEM image of fracture face showing large alumina agglomerate.

3.4. Low temperature degradation

Fig. 4 shows the results of the phase analysis of aged samples by XRD. 0Al is the only material that shows the typical sigmoidal curve of standard 3Y-TZP [8]. The plots of the alumina containing materials are similar to root functions and seem to reach a moderate saturation level rather than accelerate in the intermediate stage. Especially for 2Al-M the final monoclinic content of ~ 6 vol.% at 100 h autoclave ageing at 134°C is extremely low. The improved ageing resistance of 2Al-M compared to 2Al-C is probably related to its more homogeneous microstructure. Fig. 5 shows the MAJ plot for the three materials. The rate constants *b* (ln*b* is the ordinate intercept in Fig. 5) and the Avrami exponents (slope *m*) can be read from this linearized plot. Corresponding to the observed shape of the curve, 0Al is the only material which shows – within the margins of the standard deviation – a straight MAJ line with a slope close to 1. This is what can be expected assuming zero order (constant) progression rate of the reaction front into the bulk [11]. The Avrami exponents for the alumina containing materials are much lower.

The evolution of surface roughness vs. ageing time is shown in Fig. 6. White light interferometry images of aged surfaces (0Al and 2Al-C, 70 h ageing at 134 °C) are presented in Fig. 7.

The roughness values plotted in Fig. 6 show identical trends as the monoclinic contents shown in Fig. 4; as the volume of zirconia expands upon transformation from tetragonal to monoclinic this is evident. 2Al-M hardly shows any roughening after 100 h compared to the initial threshold of S_A = 15-20 nm. 2Al-C shows a fast increase of roughness between 1-30 h then the roughening trend tends to levels out, for the 0Al an acceleration of roughening is observed at exposition time > 70 h. A comparison of the surface structure of aged 0Al and 2Al-C shows the reason for the uncommon behaviour. In case of 0Al, the surface is almost entirely covered with a transformed layer after 70 h. In some regions, an uplift of 0.5-0.7 µm is observed. 2Al-C shows isolated transformed regions, local uplift does not exceed ~ 0.1 µm. As an Avrami exponent of ≥ 1 can only be expected during the growth regime, lower exponents can be justified if the transformation has not yet overcome the nucleation regime.

4. Discussion

Manufacturing of 3Y-TZP by stabilizer coating has been shown to be beneficial in terms of damage tolerance/frac-

Table 1. Mechanical properties of 3Y-TZP materials.

Property	Unit	0Al	2Al-C	2Al-M
Density ρ	[g/cm³]	6.09 ± 0.01	6.05 ± 0.01	6.01 ± 0.01
Hardness *HV*10	[GPa]	12.4 ± 0.2	12.2 ± 0.2	12.8 ± 0.1
Young's modulus E	[GPa]	208 ± 2	211 ± 2	205 ± 2
Bending strength σ_{4pt}	[MPa]	990 ± 130	740 ± 50	1020 ± 110
Fracture toughness K_{IC}	[MPa√m]	9.9 ± 0.4	10.9 ± 0.5	12.2 ± 0.6
Threshold K_{IO}	[MPa√m]	5.8 ± 0.4	6.6 ± 0.5	6.5 ± 0.6

ture resistance and resistance to low temperature degradation. Both effects are presumably caused by the existence of a stabilizer concentration gradient from grain boundary to the centre of the grains. TEM studies by Ohnishi [24] have shown that there is not only the usual yttria enrichment in the outer shell of the grains in the microstructure. In grains of Y-TZP sintered at moderate temperatures yttria depleted regions exist. Taking into account how the manufacturing procedure is carried out, this is quite obvious. Yttria initially covers the outside of stabilizer free zirconia grains. According to high temperature XRD data by Burger on yttria coated powder [16] the uptake of yttria and the formation of tetragonal phase takes place above the tie line (vertical t/m+c phase boundary) temperature between 1175°C and 1300°C and is completed at 1400°C. Yttria diffuses from the outside into the grains. This process is complete once the grain has reached the saturation concentration (~2.5 mol% Y_2O_3, at t/t+c phase boundary at 1350°C). Superfluous yttria has to be taken up either in the grain boundary (which can accommodate more large cations than the bulk) or stay outside and form cubic phase (large grains visible in Fig. 2). It was shown by the authors that this process is highly dynamic with respect to the consequences for the mechanical properties [17]. At the given sintering temperature of 1350°C and 1 h dwell there is a small amount of monoclinic (2%-4%) left in all three TZP materials. This residual monoclinic is probably located in the center of the grains, no indication was found of monoclinic grains in the microstructure (Fig. 2). This yttria gradient does not only leave the grain boundaries supersaturated with yttria and thus relatively invulnerable to ageing, the intragranular monoclinic puts the grains under compression from the inside and strengthens the grain boundaries. This probably leads to a shift in fracture mechanism and is most probably the main reason for the high fracture resistance. It was shown by Singh and Kern [15, 17] that the toughness of TZP made by coating technique breaks down abruptly at higher sintering temperatures, when the stabilizer redistribution is completed and the yttria gradient and the intragranular monoclinic domains are eliminated. The beneficial effect of alumina to reduce the LTD was expected and reflects the literature data, it was however quite surprising that the way of alumina addition is important and not only the amount of alumina added. In Al-C the alumina seems very unevenly distributed with results not only in poor strength but also in a lesser enhancement of ageing resistance. It is however too early to say that addition of alumina by coating is inferior

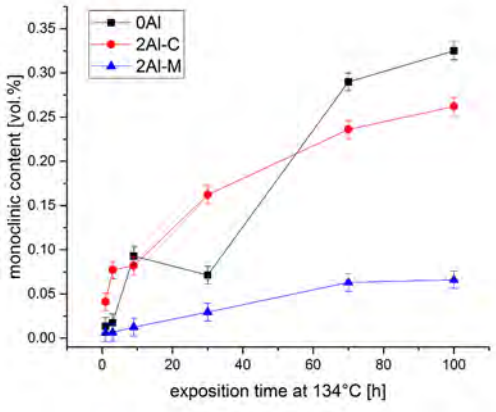

Fig. 4. Monoclinic content of TZP materials vs. exposition time at 134°C in saturated water vapour.

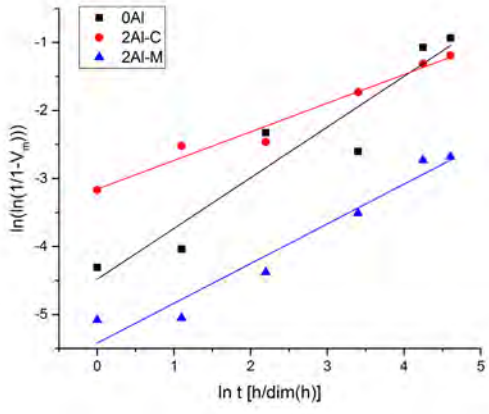

Fig. 5. Mehl-Avrami-Johnson plot of LTD kinetics at 134°C for three TZP materials.

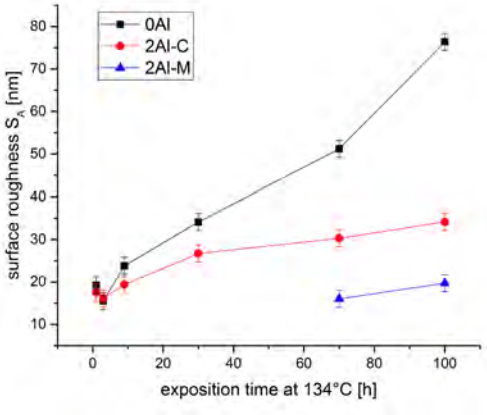

Fig. 6. Evolution of surface roughness S_A of TZP materials vs. exposition time at 134°C in saturated water vapour.

Table 2. Coefficients obtained from regression analysis of data plotted in Fig. 5.

	unit	0Al	2Al-C	2Al-M
Intercept ln *b*	-	-4.48 ± 0.21	-3.15 ± 0.37	-5.42 ± 0.11
Rate *b*	[1/h]	$1.13 \cdot 10^{-2}$	$4.29 \cdot 10^{-2}$	$4.43 \cdot 10^{-3}$
Avrami exponent *m*	-	0.75 ± 0.07	0.42 ± 0.04	0.58 ± 0.07
Correlation coefficient R^2	-	0.94	0.88	0.96
Significance level α	-	<0.01	<0.01	<0.01

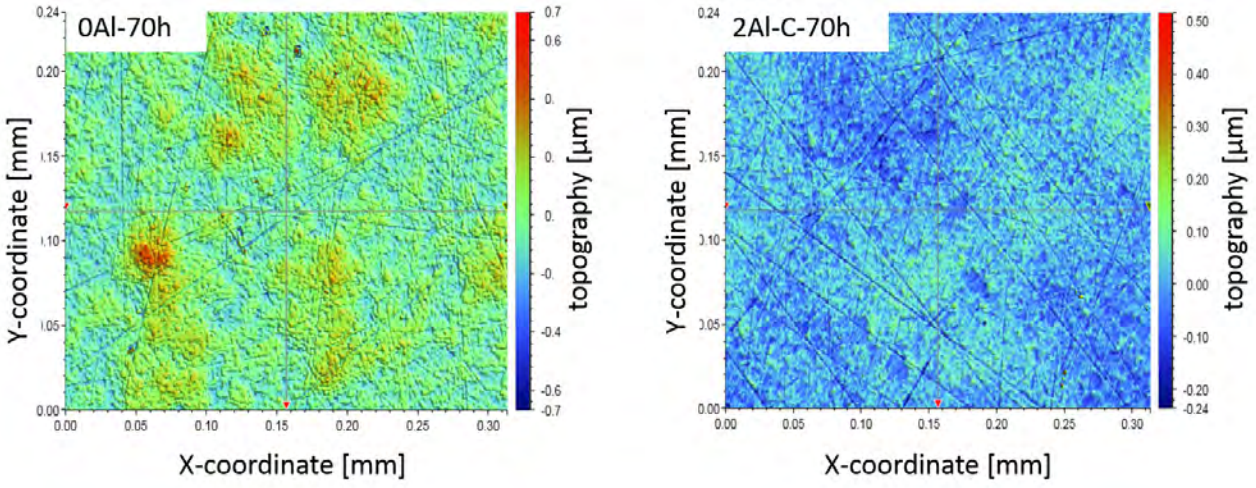

a) *b)*

Fig. 7. While light interferometry images of 0Al (a) and 2Al-C (b) TZP material after accelerated aging for 70 h at 134°C.

in general, we may state however that this first attempt was unsuccessful but that a more controlled elaboration of the powders may lead to better results. LTD is of major concern in biomedical application such as hip and knee implants in even in case of dental applications. This study provides further strong evidence that shifting from co-precipitated powders to stabilizer coated powders and application of proper processing protocols (low sintering temperature, fine grain size, full density) may provide materials with a more than sufficient LTD resistance to justify their application in the biomedical field. Moreover the TZPs made from stabilizer coated powders are much tougher and provide higher damage tolerance. The higher toughness is not only achieved by exploiting R-curve behaviour but by improving the threshold toughness. For components exposed to permanent loading the relevant coefficient besides the strength is the ratio between K_{IO}/K_{IC} [26]. For co-precipitated 3Y-TZP, K_{IO}/K_{IC} = 2.8 MPa$\sqrt{m}$ / 5 MPa$\sqrt{m}$ = 0.56. For Y-TZP from stabilizer coated powder values (Table 1) both K_{IO} and K_{IC} are improved by the same ratio so that the fatigue strength stays at the same level despite much higher damage tolerance for single catastrophic events.

5. Summary

Three different 3Y-TZP powders were manufactured by powder coating technology. Plain 3Y-TZP (0Al) showed high strength and toughness and ageing stability up to 30 h ageing time at 134°C. At longer exposition time, the ageing accelerates and the samples show a considerable increase of roughness. The introduction of alumina by mixing and milling of 0Al and 2 vol.% submicron size alumina (2Al-M) leads to the best results in terms of strength and toughness combined with the resistance to low temperature degradation. Addition of alumina as a nitrate salt together with the yttria stabilizer during the coating process (2Al-C) leads to ageing stability between 0Al and 2Al-M, high fracture resistance but inferior strength. It seems that this process is not sufficiently well engineered yet as it was found that large alumina agglomerates are formed which act as structural defects.

Acknowledgements

The authors would like to thank Prof. G. Schmitz and Dr. M. Roussel, Universität Stuttgart IMW Lehrstuhl Materialphysik for permission to use the TEM, and Mr. G. Maier and Mrs. F. Predel from Max Planck Institut Stuttgart (IS & FKF) for their assistance in XRD and SEM.

References

[1] Gupta, T. K., Bechtold, J. H., Kuznicki, R. C. Cadoff, L. H., Rossing, B. R.: Stabilization of tetragonal phase in polycrystalline zirconia, *J. Mat. Sci.*, 12, (1977), 2421-2426.

[2] Lange, F. F.: Transformation toughening – Part 3: Experimental Observations in the ZrO_2-Y_2O_3-System, *J. Mat. Sci.*, 17, (1982), 240-246.

[3] Tsukuma, K., Shimada, M.: Hot isostatic pressing of Y_2O_3 partially stabilized zirconia, *Am. Ceram. Soc. Bull.*, 64, (1985), 310-313.

[4] Kelly, P. M., Rose, L. R. F.: The martensitic transformation of ceramics - its role in transformation toughening, *Prog. Mater. Sci.*, 47, (2002), 463-557.

[5] Hannink, R. H. J., Kelly, P. M., Muddle, B. C.: Transformation Toughening in Zirconia-Containing Ceramics, *J. Am. Ceram. Soc.*, 83, 3, (2000), 461–87.

[6] Chen, M., Hallstedt, B., Gauckler, L.: Thermodynamic modeling of the ZrO_2–$YO_{1.5}$ system, *Solid State Ionics*, 170, (2004), 255–274.

[7] Li, P., Chen, I. W., Penner-Hahn, J.: Effect of Dopants on Zirconia Stabilization - An X-ray Absorption Study: I, Trivalent Dopants, *J. Am. Ceram. Soc.*, 77, (1994), 118-128.

[8] Chevalier, J., Drouin, J. M., Cales, B.: Low-Temperature Aging of Y-TZP Ceramics, *J. Am. Ceram. Soc.*, 82, 8, (1999), 2150–54.

[9] Chevalier, J., Gremillard, L.: Low-Temperature Degradation of Zirconia and Implications for Biomedical Implants, *Annu. Rev. Mater. Res.*, 37, (2007),1–32.

[10] Chevalier, J., Gremillard, L., Virkar, A., Clarke, D.: The Tetragonal-Monoclinic Transformation in Zirconia: Lessons Learned and Future Trends, *J. Am. Ceram. Soc.*, 92, 9, (2009), 1901–1920.

[11] Keuper, M., Eder, K., Berthold, C., Nickel, K. G: Direct evidence for continuous linear kinetics in the low-temperature degradation of Y-TZP, *Acta Biomaterialia*, 9, 1, (2013) 4826-35.

[12] Ross, I. M., Rainforth, W. M., McComb, D. W., Scott, A. J., Brydson, R.: The role of trace additions to yttria-tetragonal zirconia polycrystals (Y-TZP), *Scripta Materialia*, 45, (2001), 653-60.

[13] Piconi, C., Burger, W., Richter, H. G., Cittadini, A., Maccauro, G., Covacci, M., Bruzzese, N, Ricci, G. A., Marmo, E: Y-TZP ceramics for artificial joint replacements, *Biomaterials*, 19, (1998), 1489-94.
[14] Zhang, F., Vanmeensel, K., Inokoshi, M., Batuk, M., Hadermann, J., Van Meerbeek, B., Naert, I., Vleugels, J.: 3Y-TZP ceramics with improved hydrothermal degradation resistance and fracture toughness, *J. Eur. Ceram. Soc.*, 34, (2014), 2453-63.
[15] Singh, R., Gill, C., Lawson, S., Dransfield, G. P.: Sintering, microstructure and mechanical properties of commercial YTZPs, *J. Mat. Sci.*, 31, (1996), 6055-62.
[16] Burger, W., Richter, H. G., Picconi, C., Vatteroni, R., Cittadini, A. Boccalari, M: New Y-TZP powders for medical grade zirconia, *J. Mat. Sci. - Materials in Medicine*, 8, (1997), 113-118.
[17] Kern, F., Gadow, R.: Tough to brittle transition with increasing grain size in 3Yb-TZP ceramics manufactured from stabilizer coated nanopowder, *J. Ceram. Soc. Jap.*, 124, (2016), 1083-1089.
[18] Danilenko, I., Konstantinova, T., Volkova, G., Burkhovetski, V., Glazunova, V.: The Role of Powder Preparation Method in Enhancing Fracture Toughness of Zirconia Ceramics with Low Alumina Amount, *J. Cer. Sci. Techn.*, 6, (2015), 191-200.
[19] Yuan, Z. X., Vleugels, J., Van der Biest, O.: Preparation of Y_2O_3-coated ZrO_2 powder by suspension drying, *J. Mater. Sci. Lett.*, 19, (2000), 359–61.
[20] Chantikul, P., Anstis, G. R., Lawn, B. R., Marshall, D. B.: A critical evaluation of indentation techniques for measuring fracture toughness: II, strength method, *J. Am. Ceram. Soc.*, 64, 9, (1981), 539-543.
[21] Dransmann, G. W., Steinbrech, R. W., Pajares, A., Guiberteau, F., Dominguez-Rodriguez, A., Heuer, A. H.: Indentation Studies on Y_2O_3-Stabilized ZrO_2: II, Toughness Determination from Stable Growth of Indentation-Induced Cracks, *J. Am. Ceram. Soc.*, 77, 5, (1994), 1194-201.
[22] Mendelson, M. I: Average Grain Size in Polycrystalline Ceramics, *J. Am. Ceram. Soc.*, 56, 8, (1969), 443-46.
[23] Toraya, H., Yoshimura, M., Somiya, S.: Calibration curve for quantitative analysis of the monoclinic-tetragonal ZrO_2 system by X-ray diffraction, *J. Am. Ceram. Soc.*, 67, 6, (1984), C119–21.
[24] Chevalier, J., Saadaoui, M., Olagnon, C., Fantozzi, G.: Double-torsion testing a 3Y-TZP ceramic, *Ceram. Int.*, 22, (1996) ,171–177.
[25] Kern, F. Gadow, R.: Mechanical properties and low temperature degradation resistance of 2.5Y-TZP – alumina composites, *Materiały Ceramiczne /Ceramic Materials/*, 65, (2013), 258-266.
[26] Ohnishi, H., Naka, H., Sekino, T., Ikuhara, Y., Niihara, K.: Mechanical properties of 2.0-3.5 mol% Y_2O_3-stabilized zirconia polycrystals fabricated by the solid phase mixing and sintering method, *J. Ceram. Soc. Jap.*,116, (2008), 1270-1277.
[27] De Aza, A. H., Chevalier, J., Fantozzi, G., Schehl, M., Torrecillas, R.: Slow-Crack-Growth Behavior of Zirconia-Toughened Alumina Ceramics Processed by Different Methods, *J. Am. Ceram. Soc.*, 86, (2003), 115–120.

♦

Received 21 July 2017, accepted 10 August 2017.